ACS APPLIED MATERIALS & INTERFACES

Research Article

www.acsami.org

# Synthesis, Microstructure, and Cathodoluminescence of [0001]-Oriented GaN Nanorods Grown on Conductive Graphite Substrate

Fang Yuan,[†,‡] Baodan Liu,*[,‡] Zaien Wang,[†] Bing Yang,[‡] Yao Yin,[§] Benjamin Dierre,[§] Takashi Sekiguchi,[§] Guifeng Zhang,[†] and Xin Jiang*[,‡]

[†]School of Materials Science and Engineering, Dalian University of Technology, Dalian 116024, China

[‡]Shenyang National Laboratory for Materials Science, Institute of Metal Research (IMR), Chinese Academy of Sciences, No. 72 Wenhua Road, Shenyang 110016, China

[§]World Premier International (WPI) Center for Materials Nanoarchitectonics (MANA), National Institute for Materials Science (NIMS), Namiki 1-1, Tsukuba, Ibaraki, 305-0044, Japan

**ABSTRACT:** One-dimensional GaN nanorods with corrugated morphology have been synthesized on graphite substrate without the assistance of any metal catalyst through a feasible thermal evaporation process. The morphologies and microstructures of GaN nanorods were characterized by X-ray powder diffraction (XRD), scanning electron microscopy (SEM) and high-resolution transmission electron microscopy (HRTEM). The results from HRTEM analysis indicate that the GaN nanorods are well-crystallized and exhibit a preferential orientation along the [0001] direction with $Ga^{3+}$-terminated $(10\bar{1}1)$ and $N^{3-}$-terminated $(10\bar{1}\bar{1})$ as side facets, finally leading to the corrugated morphology surface. The stabilization of the electrostatic surface energy of $\{10\bar{1}1\}$ polar surface in a wurtzite-type hexagonal structure plays a key role in the formation of GaN nanorods with corrugated morphology. Room-temperature cathodoluminescence (CL) measurements show a near-band-edge emission (NBE) in the ultraviolet range and a broad deep level emission (DLE) in the visible range. The crystallography and the optical emissions of GaN nanorods are discussed.

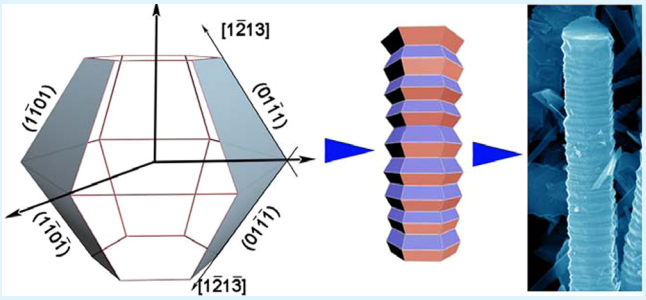


**KEYWORDS:** *GaN, nanorods, graphite, crystallography, cathodoluminescence*

## INTRODUCTION

Gallium nitride (GaN), an important semiconductor material with a band gap of 3.4 eV at room temperature, has received a great deal of attention in the past decades because of its advantageous properties such as high melting point, excellent thermal conductivity, large electron velocity, and chemical inertness, and its significant applications in high-temperature high-power electronic devices, light-emitting diodes (LED), field emitters, as well as UV photodetectors.[1−6] To date, the miniaturization of devices and the bottom-up synthetic technology have led to an increasing research interest in the fabrication of semiconductor nanostructures with various morphologies and diverse functions. Compared with their bulk counterparts, one-dimensional (1D) nanostructures may exhibit peculiar and unique properties because of their smaller size and large surface-to-volume ratio, as well as confined quantum effects. For instance, wurtzite GaN nanostructures exhibit high piezoelectric properties[7] and high spatial separation of charge carriers.[8] These important characteristics open up the possibility of using GaN nanowires as building blocks for nanogenerator[9,10] and biological sensors.[11]

Wurtzite GaN nanostructures with different morphologies such as nanowires,[12] nanobelts,[13] and nanorods[14] have been extensively fabricated by chemical vapor deposition (CVD),[1,15] molecular beam epitaxy (MBE),[8] and hydride vapor phase epitaxy (HVPE)[16] via the vapor−liquid−solid (V−L−S)[17] growth process on metal-coated (such as Ni, Fe, Au, etc.) substrates.[18] For the epitaxial growth of GaN nanowires, the substrates are critical for guiding the growth direction, morphology, and structure. So far, a variety of substrates including Si,[2,11] GaN,[19] sapphire,[14,20] diamond,[21,22] and $LiAlO_2$[23] crystals have been widely utilized for the epitaxial growth of GaN nanowires due to their lattice matching with GaN. Among these substrates, Si substrate is of great interest because of its low cost and easy processability, thus being widely used in various optoelectronic applications.[24] GaN nanostructures with different morphologies and orientations have been deposited on Si substrate by various physical and chemical methods.[12,25,26] However, the poor conductivity of Si has limited the applications of GaN nanowires in diverse fields. For example, electrochemical biosensors made of GaN nanowires generally require highly conductive substrate to

**Received:** September 10, 2013
**Accepted:** October 28, 2013
**Published:** October 28, 2013

  

transport the electrons more freely under a lower electrical field, whereas the high resistance of Si obviously depresses the sensitivity of signals and thus leads to the degradation of sensor performance. Therefore, it is essential to deposit GaN nanowires on highly conductive substrates for the purpose of improving the sensitivity of GaN-based nanodevices. Compared with Si and other substrates mentioned above, graphite is more stable at high temperature and exhibits excellent performance in electrical and thermal conductivities, and a lower thermal expansion coefficient. The deposition of bulky semiconductor materials on graphite has been investigated thirty years ago[27] and series of works have been carried out. As a typical example, multilayer graphene has been utilized as a transparent conducting electrode[28,29] for the building of high-efficiency light-emitting diodes (LEDs). On the other hand, the layered structure of graphene enables an easy removal of integrated nanodevices on various substrates.[30] In comparison with the widely used graphene, less work has been reported on the deposition of semiconductor nanostructures on graphite substrate. Theoretical studies on the growth of GaN film on graphite[31] and vapor phase deposition of GaN film on graphite[26] have been also reported. The advantage of graphite substrate for the growth of GaN nanostructures is as following: (1) the lattice mismatch between [0001]-oriented wurtzite GaN and graphite is smaller enough, and thus a smaller lattice stress of GaN nanostructures and a higher crystallinity can be expected; (2) the excellent electric conductivity of graphite can allow the direct device integration of GaN nanostructures on graphite substrate; (3) GaN nanostructures grown on graphite can be selectively transferred to other substrates because of the easy removal of graphite layered structure. However, the growth of GaN nanostructures on graphite substrate through a feasible CVD process has been rarely reported.

In this paper, we reported the successful fabrication of large-scale GaN nanorods on graphite substrate via a simple and low-cost CVD process without involving any metal catalyst. The GaN nanorods exhibit typical characteristics of single crystal, corrugated morphology and a hexagonal cross section. High-resolution transmission electron microscopy (HR-TEM) analyses have been carried out on the microstructural and crystallographic studies and it was found that the GaN nanorods have alternate $\{10\bar{1}1\}$ polar facets along the side surfaces. The reduction of the electrostatic surface energy from these alternating $\{10\bar{1}1\}$ polar surfaces plays a key role in the formation of such corrugated GaN.

## EXPERIMENTAL SECTION

GaN nanorods grown on graphite substrate were obtained through a simple CVD process as described in our previous work.[2] High-purity $Ga_2O_3$ powders (Sinopharm Chemical Reagent Co. Ltd., purity >99.99%) were first loaded into a cylindrical $Al_2O_3$ boat as precursors and then inserted into a small quartz tube (30 mm in diameter and 100 cm in length) for preventing impurity invasion. The smaller quartz tube with $Al_2O_3$ boat was then inserted into a large quartz tube (45 mm in diameter and 160 cm in length), which was heated by a conventional horizontal resistance furnace. Graphite substrate with smooth surface (20 × 20 $mm^2$) was put at the gas outlet of the inner smaller quartz tube. After connecting the quartz tube with high-purity flowing Ar gas, the furnace was first heated to 473K under the protection of 100 standard cubic centimeter per minute (sccm) Ar and then $NH_3$ gas with a flowing rate of 100 sccm was induced to replace Ar gas as nitrogen source. The temperature was continuously increased to 1373 K and maintained at this temperature for 30 min. After the reaction, the growth chamber was naturally cooled to room temperature in Ar flow and large-scale yellow powderlike layers were densely grown on graphite substrate.

The phase and purity of as-grown GaN nanorods were examined by a Rigaku RINT 2000 X-ray powder diffractometer (XRD) with Cu K$\alpha$ radiation, operating at 40 kV and 40 mA. The morphology of the as-synthesized samples was measured by a Zeiss Supra 55 scanning electron microscope (SEM). The microstructure and composition of the samples were characterized and analyzed using a Tecnai $G^2$ F20 high-resolution field emission transmission electron microscope (FETEM) equipped with an X-ray energy dispersive spectrometer (EDS). For the optical measurements, the cathodoluminescence (CL) spectroscopy of GaN nanorods was directly performed on the GaN nanorods grown on graphite substrate and on those dispersed on Cu TEM grids in a field-emission SEM (Hitachi S4300) equipped with a CL system at an accelerated voltage of 15 kV.

## RESULTS AND DISCUSSIONS

Figure 1 shows the XRD pattern of GaN nanorods grown on graphite substrate. The diffraction peaks at $2\theta$ = 32.4, 34.6, 36.8, 48.1, and 57.7° can be well-indexed to a standard wurtzite-type hexagonal GaN (space group: $P63mc$) with lattice constants of $a$ = 3.189 Å and $c$ = 5.18 Å, whereas these peaks appearing at $2\theta$ = 42.2, 44.2, and 50.5° are from graphite substrate. In addition, a weak peak centered at 39.8° can be noticed, and this peak can be roughly indexed to $Ga_2O_3$. The formation of $Ga_2O_3$ is possible during the synthesis of GaN nanorods because some residual oxygen may exist in the reaction chamber. Meanwhile, the diffraction peaks from C-containing impurity compounds were yet not observed. It is well-known that GaN crystal can exist in either stable wurtzite (WZ, hexagonal) or metastable zinc-blende (ZB, cubic) structures.[32] The crystallographic difference between the two structures only comes from the atom ordering sequence. Under given growth condition, WZ phase can coexist with metastable ZB phase in GaN nanowires.[33] The absence of any metastable ZB-GaN diffraction peaks in XRD pattern further demonstrated that the as-synthesized GaN nanorods are crystallized in WZ structure. The GaN nanostructures densely deposited on graphite substrate exhibited obvious yellow color. To investigate their morphology, SEM observation with an accelerated voltage of 10 kV was utilized. Figure 2a shows the low-magnification SEM image of as-synthesized product and one can clearly see that large-yield GaN nanostructures with a typical rodlike morphology are randomly grown on the

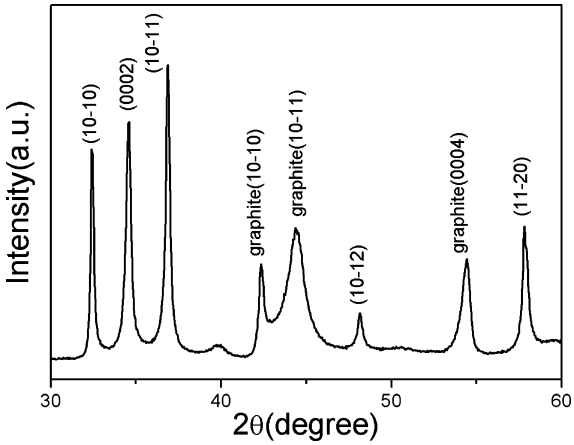


**Figure 1.** X-ray diffraction pattern of GaN nanorods grown on a graphite substrate.

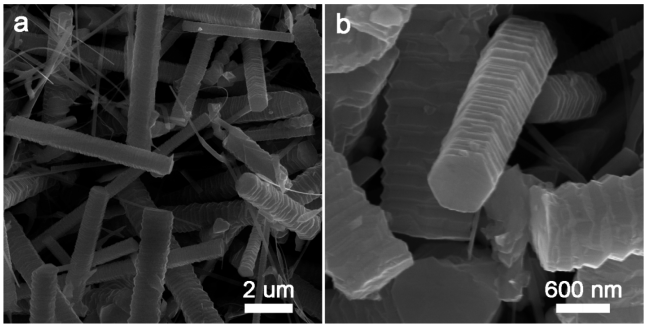


**Figure 2.** (a) Low-magnification SEM image of the as-synthesized GaN nanorods; (b) high-resolution SEM image of nanorods with hexagonal cross-section.

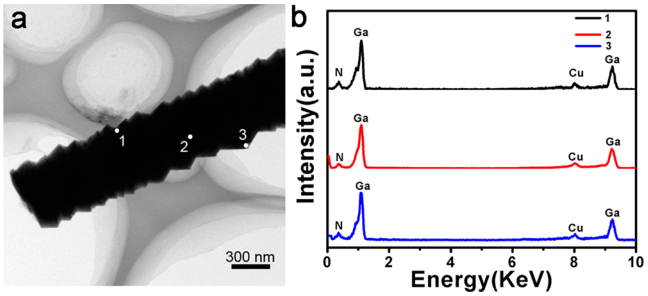


**Figure 3.** (a) Representative bright-field TEM image of an individual GaN nanorod and (b) its corresponding EDS spectra collected from three different areas labeled with (1, 2, and 3).

graphite substrate. Occasionally, a small amount of wirelike GaN nanostructures can also be found. Further observations show that the GaN nanorod exhibits a cylindrical shape with a hexagonal cross-section and zigzag morphology. Statistical investigations on numerous samples show that the average diameter of GaN nanorods ranged from 400 to 800 nm and the length of GaN nanorods can be up to tens of micrometers. Figure 2b displays a representative high-magnification SEM image of GaN nanorods with hexagonal cross-section, which gives a clear view of the straight nanorods with coarse and corrugated side surfaces. The hexagonal tip-end with smooth flatness can be clearly observed. Additionally, from the hexagonal cross-section, it can also be assumed that the GaN nanorods are oriented along the *c*-axis of WZ-GaN. However, compared with GaN nanostructures grown on epitaxial substrate, the growth direction of GaN nanorods is not perpendicular to the graphite substrate and all the GaN nanorods are randomly distributed on the graphite surface, which is consistent with the diffraction peaks in XRD patterns. Possible reasons for the random growth of GaN nanorods may arise from the fact that the graphite layers on the top surface have been abraded during the grinding of graphite surface by sandpaper. As a result, the graphite surface is atomically not as flat as chemically polished sapphire and thus GaN nanorods can randomly nucleate and crystallize at the scratched surface. Different from diameter-modulated nanostructures synthesized via metal-assisted thermal evaporation route,[34,35] no catalyst nanoparticle is found on the tip-end of GaN nanorods from the high-magnification SEM image (Figure 2b), suggesting that the formation of GaN nanorods may follow the well-known vapor−solid (V−S) mechanism.[36]

The chemical composition and possible impurity contamination of as-synthesized GaN nanorods were further studied. Figure 3a displays a typical low-magnification bright field TEM image of an individual GaN nanorod suspending on the TEM grid. The corrugated surface of GaN nanorod with periodic diameter variation can be confirmed again. Considering that the GaN nanorods are synthesized on graphite and the carbon contamination is possible,[37] it is essential to investigate the chemical composition of as-synthesized GaN nanorods through high-resolution EDS analysis. To confirm the composition difference within the GaN nanorod, EDS measurements using a small electron beam size were performed at three representative areas, i. e.; the concave surface ("1"); the rod body ("2"); and the protruding edge ("3"). Figure 3b shows the corresponding EDS spectra of the three areas "1", "2", and "3". It can be seen that only N and Ga signals are detected from the three areas of GaN nanorod within the resolution limit of EDS, and the O peak from residual oxygen and $Ga_2O_3$ phase was not found, proving that the GaN nanorods are of high purity. The Cu peaks in the EDS spectra come from the TEM grid used. On the basis of the statistical analysis results of EDS data, it can be assumed that the GaN nanorods are slightly Ga-rich (Ga:N ≈ 1:0.92). Interestingly, no trace of elemental C signals is detected (see Figure 3b) though the GaN nanorods are nucleated on the graphite surface. The absence of C peak in EDS spectra further suggests that the concentration of carbon incorporated into GaN crystal is rather lower. Details on the microstructure and crystallinity of GaN nanorods are further obtained with high-resolution TEM analysis. Figure 4a shows a typical bright-field TEM image of an individual GaN nanorod with zigzag morphology surface and a diameter of ∼750 nm. It explicitly shows that the GaN nanorod has a periodic segment and diameter fluctuation along the growth direction. The edge surfaces of the protruding tips are always parallel each other and these edge planes can be further confirmed as $(10\bar{1}1)$ and $(10\bar{1}\bar{1})$ planes of a WZ-GaN by HRTEM analysis. The angles between the neighboring surfaces of a concave and a convex are roughly measured to be 117.9 and 119° (as marked in Figure 4a), which are slightly deviated from the standard values of $(10\bar{1}1)$ and $(10\bar{1}\bar{1})$ planes. The angle deviation comes from the tilting of GaN nanorod suspending on Cu grid during TEM observation. The flatness of the GaN nanorod tip-end suggests again that its nucleation and crystallization are realized without the assistance of any catalyst and a V−S process is involved in its formation. To evaluate the crystal quality and possible structural defects of GaN nanorods grown on graphite substrate, HRTEM analyses and the corresponding fast Fourier transformation (FFT) pattern are utilized to study their structure and crystalline orientation. The concave and convex edges of several GaN nanorods are examined for a general study of the crystallinity. Images b and d in Figure 4 are the typical HRTEM images of the selected areas "1" and "2" shown in Figure 4a. The two HRTEM images are taken along the zone axis of $[\bar{1}2\bar{1}0]$. The clear lattice fringes of the crystal and well arranged atom ordering confirm that the GaN nanorods are single-crystalline and well-crystallized. Interestingly, the typical defects such as microtwins and stacking faults are not observed in all the GaN nanorods studied. In addition, the ZB-phase of GaN is not yet observed. The *d*-spacing of the lattice fringes measured from the HRTEM images is 0.52 nm, matching well with the (0001) plane interspacing of hexagonal wurtzite GaN structure. The lattice spacing parallel to side surface is 0.24 nm, in good agreement with the *d*-spacing of $(10\bar{1}1)$ lattice plane. The angle between two side surface planes shown in Figure 4b

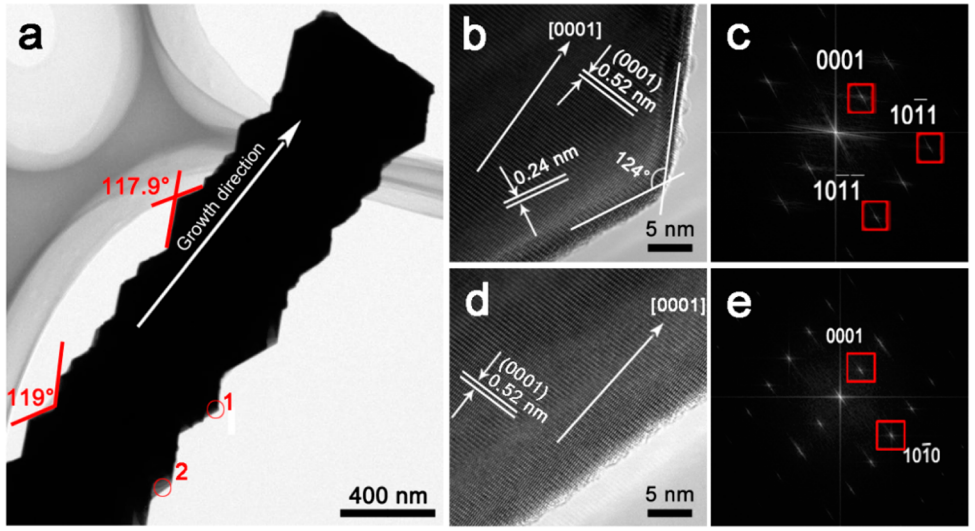


**Figure 4.** (a) Representative low-magnification bright-field TEM image of an individual GaN nanorod; (b, d) high-resolution TEM images of selected areas "1" and "2" shown in a; and (c, e) their corresponding fast Fourier transformed (FFT) patterns.

is 124°, in consist with regular value of (10$\bar{1}$1) and (10$\bar{1}\bar{1}$) planes. Therefore, the periodic parallel surfaces shown in Figure 4a can be identified as (10$\bar{1}$1) and (10$\bar{1}\bar{1}$) planes. The corresponding FFT patterns of the HRTEM images (Figure 4c, e) also show succinct diffraction spots, demonstrating again that the GaN nanorods synthesized on graphite are single crystal and orient along the [0001] direction.

It is interesting that the GaN nanorods grown on graphite substrate via a V−S process show periodic corrugated surfaces rather than the commonly observed round or hexagonal prism-like morphology,[12] and such morphology was rarely observed in CVD GaN nanostructures. The repeat of alternating concave and convex edge surfaces represents a given crystallographic relationship in WZ-GaN. To elucidate the crystallography and possible formation process, we plotted the schematic illustration of two connected truncated hexagonal cones in Figure 5a. The neighboring two hexagonal cones that comprise

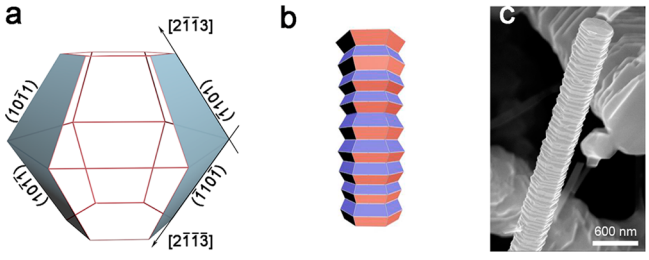


**Figure 5.** (a) Schematic of a crystal unit of the GaN nanorod with {10$\bar{1}$1}and {0001} planes enclosed; (b) schematic diagram of a GaN nanorod comprising of continuous crystal unit; (c) high-resolution SEM image of an individual GaN nanorod with hexagonal cross-section.

a basic crystal unit of the GaN nanorod have hexagonal cross-section along the [0001] growth direction, with the up and down surfaces being (0001) and (000$\bar{1}$) planes and the two tilting side surfaces being $Ga^{3+}$-terminated {10$\bar{1}$1} and $N^{3-}$-terminated {10$\bar{1}\bar{1}$}.[34] The angle of 117° between [2$\bar{1}\bar{1}$3] and [2$\bar{1}\bar{1}$3] is also in good agreement with the observed values ranging from 117 to 124° in Figure 4a. The linking of dozens of such crystal units along the *c*-axis will form the corrugated morphology, as schematically plotted in Figure 5b and presented in Figure 5c for an actual GaN nanorod. From these crystallographic analyses, we can further confirm that the side facets of GaN nanorods are {10$\bar{1}\bar{1}$} planes and the periodic appearing of (10$\bar{1}$1) and (10$\bar{1}\bar{1}$) finally leads to the formation of corrugated morphology, as observed in 1D hexagonal wurtzite stacked-cone and zigzag AlN,[34] ZnO,[35] and InN[38] nanostructures.

In the present case, the GaN nanorod with [0001] orientation and with {10$\bar{1}$1} side planes are synthesized on mechanically ground graphite. Based on previous works on zigzag GaN nanostructures[39,40] and our structural analyses, it is concluded that the formation of corrugated morphology of GaN nanorods with (10$\bar{1}$1) and (10$\bar{1}\bar{1}$) planes as the side facets can be as a result of the reduction of the electrostatic interaction energy, which is realized through the alternation of positive and negative charges on $Ga^{3+}$-terminated {10$\bar{1}$1} and $N^{3-}$-terminated {10$\bar{1}\bar{1}$} planes. Here, a tentative growth model is proposed for illustrating the formation process and mechanism of GaN nanorods with corrugated morphology. In contrast with the catalytic growth of ZnO nanostructures on graphitic surfaces,[41] no metal nanoparticle was observed at the end of GaN nanorods by SEM and TEM observations. The mechanical defects such as steps, trenches, and ledges[30] in the graphitic surfaces play a key role in the nucleation of GaN nanorods. The Ga atoms can be easily trapped by these sites and then react with ammonia at high temperature to form the first several layers of WZ-GaN crystal on graphite surface. It should be noted that all the atoms to form the initial GaN layers are stacked in the c-plane of WZ-GaN with a hexagonal shape via a self-assembled process without the assistance of any metal catalyst, and the depositions of Ga and N atoms can be repeated on previously formed GaN layer via homoepitaxial growth, as schematically described in Figure 6a. It should be also mentioned that the deposition rate of GaN layer along the *c*-axis direction is much faster than that of the side surface. In addition, the atom numbers gradually decrease with the deposition of GaN from the initial layer to the last one in a truncated hexagonal cone. As a result, the size of (0001) surface gradually decreases and the side facets {10$\bar{1}$1} or {10$\bar{1}\bar{1}$} planes appear to form the hexagonal cone (Figure 6b). Because the

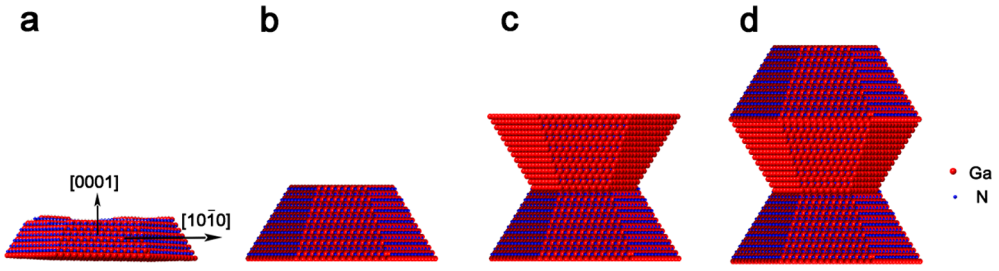


**Figure 6.** Schematic diagram showing the crystallization and subsequent growth process of GaN nanorods: (a) the initial growth stage, reflecting the GaN nanorod grows preferentially along the [0001] direction; (b, c) formation stages of Ga-terminated $\{10\bar{1}1\}$ and N-terminated $\{10\bar{1}\bar{1}\}$ side facets; (d) repeated formations of Ga-terminated $\{10\bar{1}1\}$ and N-terminated $\{10\bar{1}\bar{1}\}$ side facets that lead to the final GaN nanorods with corrugated morphology.

$Ga^{3+}$-terminated $\{10\bar{1}1\}$ and $N^{3-}$-terminated $\{10\bar{1}\bar{1}\}$ planes have different polarities and possess finite charges and dipole moments, which will give rise to positive and negative electrostatic surface energy. To keep the overall energy preferentially stable, the total surface free energy including the electrostatic surface energy and the surface energy should be minimized. When $\{10\bar{1}1\}$ (or $\{10\bar{1}\bar{1}\}$) surface planes crystallize to a certain point (Figure 6b), the dipole moment and the electrostatic surface energy will increase and induce the crystal system energetically instable. To minimize the dipole moment and reduce the electrostatic surface energy, the $\{10\bar{1}\bar{1}\}$ (or $\{10\bar{1}1\}$) side facets with an opposite polarity will be gradually formed to balance the system energy, as shown in Figure 6c. The alternation of the dipole moments and the change of the electrostatic surface energy will lead to the repeated formation of $Ga^{3+}$-terminated $\{10\bar{1}1\}$ and $N^{3-}$-terminated $\{10\bar{1}\bar{1}\}$ side facets along the *c*-axis direction and finally produce the 1D GaN nanostructures with corrugated morphology, as schematically illustrated in Figure 6d.

With a wide band gap of 3.4 eV, GaN has extensive and technologically important applications in a wide range of optics and optoelectronics. Nanostructured GaN holds unparallel advantages and optical properties compared with their counterparts in bulk. Especially, the luminescence emissions of GaN nanostructures are strongly dependent on their particular sizes, orientations, and growth parameters. To study the optical properties of GaN nanorods grown on graphite substrate, the CL spectra of GaN nanorods with coarse corrugated surfaces were measured at room temperature under an applied accelerating voltage ($V_a$) of 15 kV. Figure 7 depicts a representative CL spectrum randomly collected from a GaN nanorod in the range of 200−800 nm. It can be seen that the GaN nanorod exhibits a weak emission centered at 380 nm and a broad peak in visible light range centered at 630 nm respectively. Similar to the luminescence of most GaN nanostructures, the 380 nm ultraviolet (UV) emission is generally considered as the near-band-edge emission (NBE) and can be assigned to the recombination of free excitons through a donor-to-valence-band transition,[42−44] whereas the strong luminescence peak is regarded as a deep level emission (DLE) in GaN. Compared to the intrinsic band-edge emission at 370 nm of bulky GaN,[45] the NBE peak of GaN nanorods exhibit an obvious red-shift, which could be associated with possible carbon impurity contamination[37,46] during the nucleation and crystallization of GaN crystal on graphite substrate. It is inevitable to completely isolate the incorporation of carbon in GaN crystal at a rather high temperature. Therefore, more or less carbon atoms will be involved in the GaN lattices as impurities. The content of carbon contamination should be under the resolution of EDS measurement. The broad peak centered at 630 nm can be attributed to some Ga or N vacancies or a related complex in line with the results of early studies on GaN.[47] To investigate the uniformity of GaN luminescence, we also studied the position-dependent CL spectra. As presented in Figure 8a, three GaN nanorods with

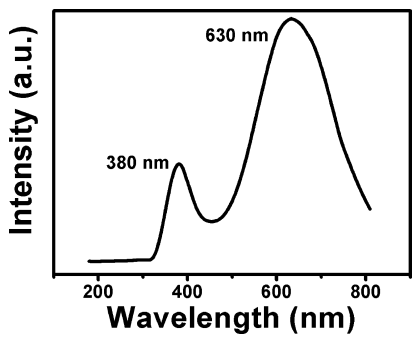


**Figure 7.** Typical CL spectrum of a GaN nanorod in the range of 200−800 nm.

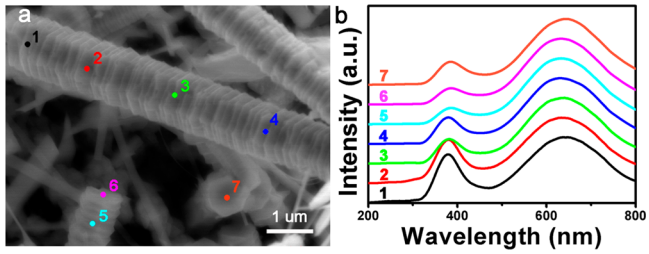


**Figure 8.** (a) SEM image of GaN nanorods random distributing on the graphite surface and the positions for CL collection; (b) the corresponding CL spectra taken from the seven areas of GaN nanorods using a "point" mode.

the same corrugated morphologies and different diameters are selected and the CL spectra are collected from either the side surfaces or the flat tip in point mode. The normalized CL spectra collected from seven different spots labeled as 1−7 are plotted in Figure 8b. It can been seen that only two emission peaks in the UV and visible light ranges are presented in all the CL spectra, similar to the CL spectra randomly collected (Figure 7). Additionally, the peak at 380 nm for the spots 1−4 did not show obvious red-shift, but the peaks for spot 5−7 are slightly shifted. This peak shift may come from the negligible composition difference from sample to sample. The excellent

luminescence and large aspect ratio of GaN nanorods, together with the superior conductivity of graphite, will enable the functional surface modification of GaN nanorods using electrochemistry methods and exploration of their promising applications in nano-optoelectronic and biorelated fields.

## CONCLUSIONS

In summary, single-crystalline WZ-GaN nanorods with corrugated morphology surfaces have been directly synthesized on graphite surface via a catalyst-free CVD process. GaN nanorods have preferential orientation along the *c*-axis of a hexagonal WZ structure. The minimizing of the total surface free energy and electrostatic surface energy induces the appearing of periodic repeat of $Ga^{3+}$-terminated$\{10\bar{1}1\}$ and $N^{3-}$-terminated $\{10\bar{1}\bar{1}\}$ side facets and finally leads to the hexagonal coarse corrugated morphology. The GaN nanorods also exhibit a NBE emission in the UV range and a strong broad luminescence in the visible range. The position-dependent CL measurements indicate that the GaN nanorods grown on graphite substrate have uniform luminescence for both 380 and 630 nm emissions. These merits of GaN nanorods in crystallinity and luminescence, as well as the advantage of graphite substrate in conductivity, will make GaN nanorods find promising applications in individual GaN-based optoelectronic devices and biorelated fields.

## AUTHOR INFORMATION


### Corresponding Authors

*E-mail: baodanliu@imr.ac.cn.

*E-mail: xjiang@imr.ac.cn.

### Author Contributions

These authors contributed equally.


### Notes

The authors declare no competing financial interest.

## ACKNOWLEDGMENTS

B.D.L. thanks the National Nature Science Foundation of China and Liaoning Province (Grants 51102034 and 201204486) and the Knowledge Innovation Program of Institute of Metal Research (IMR), Chinese Academy of Science (CAS) (Grant Y2NCA111A1) for the support of this work.

## REFERENCES


(1) Yan, R. X.; Gargas, D.; Yang, P. D. *Nat Photonics* **2009**, *3*, 569−576.

(2) Liu, B.; Hu, T.; Wang, Z.; Liu, L.; Qin, F.; Huang, N.; Jiang, X. *Cryst. Res. Technol.* **2012**, *47*, 207−212.

(3) Gonzalez-Posada, F.; Songmuang, R.; Den Hertog, M.; Monroy, E. *Nano Lett.* **2012**, *12*, 172−176.

(4) Pearton, S. J.; Zolper, J. C.; Shul, R. J.; Ren, F. *J. Appl. Phys.* **1999**, *86*, 1−78.

(5) Chen, Z.; Cao, C.; Li, W. S.; Surya, C. *Cryst. Growth. Des.* **2009**, *9*, 792−796.

(6) Wu, H.; Sun, Y.; Lin, D.; Zhang, R.; Zhang, C.; Pan, W. *Adv. Mater.* **2009**, *21*, 227−231.

(7) Song, J.; Zhou, J.; Wang, Z. L. *Nano Lett.* **2006**, *6*, 1656−1662.

(8) Calarco, R.; Marso, M.; Richter, T.; Aykanat, A. I.; Meijers, R.; A, V. D. H.; Stoica, T.; Luth, H. *Nano Lett.* **2005**, *5*, 981−984.

(9) Huang, C. T.; Song, J. H.; Lee, W. F.; Ding, Y.; Gao, Z. Y.; Hao, Y.; Chen, L. J.; Wang, Z. L. *J. Am. Chem. Soc.* **2010**, *132*, 4766−4771.

(10) Wang, Z. L.; Song, J. *Science* **2006**, *312*, 242−246.

(11) Kum, H.; Heo, J.; Jahangir, S.; Banerjee, A.; Guo, W.; Bhattacharya, P. *Appl. Phys. Lett.* **2012**, *100*, 182407−182407−4.

(12) Duan, X.; Lieber, C. M. *J. Am. Chem. Soc.* **2000**, *122*, 188−189.

(13) Bae, S. Y.; Seo, H. W.; Park, J.; Yang, H.; Park, J. C.; Lee, S. Y. *Appl. Phys. Lett.* **2002**, *81*, 126−128.

(14) Kim, H. M.; Kim, D. S.; Park, Y. S.; Kim, D. Y.; Kang, T. W.; Chung, K. S. *Adv. Mater.* **2002**, *14*, 991−993.

(15) Chen, X.; Xu, J.; Wang, R. M.; Yu, D. *Adv. Mater.* **2003**, *15*, 419−421.

(16) Seryogin, G.; Shalish, I.; Moberlychan, W.; Narayanamurti, V. *Nanotechnology* **2005**, *16*, 2342−2345.

(17) Wagner, R. S.; Ellis, W. C. *Appl. Phys. Lett.* **1964**, *4*, 89−90.

(18) Chen, X.; Li, J.; Cao, Y.; Lan, Y.; Li, H.; He, M.; Wang, C.; Zhang, Z.; Qiao, Z. *Adv. Mater.* **2000**, *12*, 1432−1434.

(19) Hersee, S. D.; Sun, X.; Wang, X. *Nano Lett.* **2006**, *6*, 1808−1811.

(20) Yoo, J.; Hong, Y.-J.; An, S. J.; Yi, G.-C.; Chon, B.; Joo, T.; Kim, J.-W.; Lee, J.-S. *Appl. Phys. Lett.* **2006**, *89*, 043124−043124−3.

(21) Schuster, F.; Furtmayr, F.; Zamani, R.; Magen, C.; Morante, J. R.; Arbiol, J.; Garrido, J. A.; Stutzmann, M. *Nano Lett.* **2012**, *12*, 2199−2204.

(22) Hirama, K.; Taniyasu, Y.; Kasu, M. *Appl. Phys. Lett.* **2011**, *98*, 162112−162112−3.

(23) Kuykendall, T.; Pauzauskie, P. J.; Zhang, Y.; Goldberger, J.; Sirbuly, D.; Denlinger, J.; Yang, P. *Nat. Mater.* **2004**, *3*, 524−528.

(24) Yang, P.; Yan, R.; Fardy, M. *Nano Lett.* **2010**, *10*, 1529−1536.

(25) Maeda, K.; Takata, T.; Hara, M.; Saito, N.; Inoue, Y.; Kobayashi, H.; Domen, K. *J. Am. Chem. Soc.* **2005**, *127*, 8286−8287.

(26) Shimada, S.; Taniguchi, R. *J. Cryst. Growth.* **2004**, *263*, 1−3.

(27) Chu, T. L.; Mollenkopf, H. C.; Chu, S. S. C. *J. Electrochem. Soc.* **1976**, *123*, 106−110.

(28) Kim, B.-J.; Lee, C.; Jung, Y.; Hyeon Baik, K.; Mastro, M. A.; Hite, J. K.; Eddy, C. R.; Kim, J. *Appl. Phys. Lett.* **2011**, *99*, 143101−143101−3.

(29) Jo, G.; Choe, M.; Cho, C. Y.; Kim, J. H.; Park, W.; Lee, S.; Hong, W. K.; Kim, T. W.; Park, S. J.; Hong, B. H.; Kahng, Y. H.; Lee, T. *Nanotechnology* **2010**, *21*, 175201−175201−6.

(30) Munshi, A. M.; Dheeraj, D. L.; Fauske, V. T.; Kim, D. C.; van Helvoort, A. T.; Fimland, B. O.; Weman, H. *Nano Lett.* **2012**, *12*, 4570−4576.

(31) Ishii, A.; Tatani, T.; Asano, H.; Nakada, K. *Phys. Status Solidi C* **2010**, *7*, 347−350.

(32) As, D. J.; Schmilgus, F.; Wang, C.; Schöttker, B.; Schikora, D.; Lischka, K. *Appl. Phys. Lett.* **1997**, *70*, 1311−1313.

(33) Jacopin, G.; Rigutti, L.; Largeau, L.; Fortuna, F.; Furtmayr, F.; Julien, F. H.; Eickhoff, M.; Tchernycheva, M. *J. Appl. Phys.* **2011**, *110*, 064313−064313−5.

(34) Wang, H.; Xie, Z.; Wang, Y.; Yang, W.; Zeng, Q.; Xing, F.; An, L. *Nanotechnology* **2009**, *20*, 025611−025611−6.

(35) Glushenkov, A. M.; Zhang, H.; Zou, J.; Lu, G. Q.; Chen, Y. *J. Cryst. Growth* **2008**, *310*, 3139−3143.

(36) Sahoo, P.; Dhara, S.; Amirthapandian, S.; Kamruddin, M.; Dash, S.; Panigrahi, B. K.; Tyagi, A. K. *Cryst. Growth. Des.* **2012**, *12*, 2375−2381.

(37) Zhang, R.; Kuech, T. F. *Appl. Phys. Lett.* **1998**, *72*, 1611−1613.

(38) Ji, X.; Cheng, S.; Hu, H.; Li, H.; Wu, Z.; Yan, P. *AIP Adv.* **2012**, *2*, 022150−022150−7.

(39) Xie, X.; Wang, G. Z.; Shao, Z. B.; Li, D. P. *J. Phys. Chem. C* **2009**, *113*, 14633−14637.

(40) Zhou, X. T.; Sham, T. K.; Shan, Y. Y.; Duan, X. F.; Lee, S. T.; Rosenberg, R. A. *J. Appl. Phys.* **2005**, *97*, 104315−14315−6.

(41) Kumar, B.; Lee, K. Y.; Park, H. K.; Chae, S. J.; Lee, Y. H.; Kim, S. W. *ACS Nano* **2011**, *5*, 4197−4204.

(42) Grieshaber, W.; Schubert, E. F.; Goepfert, I. D.; Karlicek, R. F.; Schurman, M. J.; Tran, C. *J. Appl. Phys.* **1996**, *80*, 4615−4620.

(43) Chen, G. D.; Smith, M.; Lin, J. Y.; Jiang, H. X.; Salvador, A.; Sverdlov, B. N.; Botchkarv, A.; Morkoc, H. *J. Appl. Phys.* **1996**, *79*, 2675−2683.

(44) Qiu, H.; Cao, C.; Zhu, H. *Mater. Sci. Eng., B* **2007**, *136*, 33−36.

(45) Liu, B.; Bando, Y.; Tang, C.; Shen, G.; Golberg, D.; Xu, F. *Appl. Phys. Lett.* **2006**, *88*, 093120−093120−3.

(46) Cao, J.; Pavlidis, D.; Eisenbach, A.; Philippe, A.; Bru-Chevallier, C.; Guillot, G. *Appl. Phys. Lett.* **1997**, *71*, 3880−3882.
(47) Suski, T.; Perlin, P.; Teisseyre, H.; Leszczyński, M.; Grzegory, I.; Jun, J.; Boćkowski, M.; Porowski, S.; Moustakas, T. D. *Appl. Phys. Lett.* **1995**, *67*, 2188−2190.